

Interpolatory \mathcal{H}_∞ Model Reduction

Garret Flagg, Christopher Beattie, Serkan Gugercin

Department of Mathematics, Virginia Tech.

Blacksburg, VA, 24061-0123

e-mail: `{flagg,beattie,gugercin}@math.vt.edu`

January 27, 2024

Abstract

We introduce an interpolation framework for \mathcal{H}_∞ model reduction founded on ideas from optimal- \mathcal{H}_2 interpolatory model reduction, realization theory, and complex Chebyshev approximation. We propose a method that can be applied effectively in large-scale settings with the main cost being (typically) sparse linear solves. Several numerical examples illustrate that our approach will produce high fidelity reduced-order models that consistently exhibit better \mathcal{H}_∞ performance than those produced by balanced truncation; often they are as good as (and occasionally better than) those produced by optimal Hankel norm approximation; and in all cases these reduced models can be produced at far lower cost.

1 Introduction

The need for high accuracy mathematical models in problems involving simulation and control often results in dynamical systems described by a large number of differential equations. Working with such large-scale systems can easily place overwhelming demands on computational resources, a problem which model reduction methods seek to alleviate by approximating the original model with another model consisting of far fewer (but carefully crafted) differential equations. Strategies for carrying out this approximation should be both efficient and accurate. For an overview of model reduction, see [1].

We consider here single-input/single-output (SISO) linear dynamical systems given in state-space form as:

$$\mathbf{E}\dot{\mathbf{x}}(t) = \mathbf{A}\mathbf{x}(t) + \mathbf{b}u(t), \quad y(t) = \mathbf{c}^T \mathbf{x}(t) + d u(t), \quad (1)$$

where $\mathbf{E}, \mathbf{A} \in \mathbb{R}^{n \times n}$, $\mathbf{b}, \mathbf{c} \in \mathbb{R}^n$ and $d \in \mathbb{R}$. \mathbf{E} is assumed to be nonsingular throughout, although our approach extends without difficulty to cases where \mathbf{E} is singular with $\text{nullity}(\mathbf{E}) = \text{nullity}(\mathbf{E}^2)$ (that is, 0 is a nondefective eigenvalue for \mathbf{E}). Respectively, $\mathbf{x}(t) \in \mathbb{R}^n$ are the *states*; $u(t) \in \mathbb{R}$ is the *input*; and $y(t) \in \mathbb{R}$ is the *output* of the dynamical system in (1). The *transfer function* of the system is

$$H(s) = \mathbf{c}^T (s\mathbf{E} - \mathbf{A})^{-1} \mathbf{b} + d,$$

defined for $s \in \mathbb{C}$. In accord with standard convention, we denote both the system and its transfer function by $H(s)$. We assume that $H(s)$ is both controllable and observable. The *order* of $H(s)$ is the number of poles it possesses, counting multiplicity. Since \mathbf{E} is nonsingular, all poles of $H(s)$ are finite and since $H(s)$ is controllable and observable, the order of $H(s)$ is identical to the dimension of the state vector \mathbf{x} (e.g., n for the system in (1)).

We denote the set of rational functions of order at most k which are bounded and analytic in the closed right half of the complex plane by \mathcal{H}_∞^k , and we assume in all that follows that $H \in \mathcal{H}_\infty^n$. The \mathcal{H}_∞ norm of H is defined as

$$\|H\|_{\mathcal{H}_\infty} = \max_{\omega \in \mathbb{R}} |H(j\omega)|. \quad (2)$$

If the input function, $u(t)$, is square integrable, $\|u\|_{L^2} = \left(\int_0^\infty |u(t)|^2 dt \right)^{\frac{1}{2}} < \infty$, then the output function, $y(t)$, of (1) will be square integrable as well; u and y have Fourier transforms $\hat{u}, \hat{y} \in L^2(\mathbb{R})$ that are related according to $\hat{y}(\omega) = H(j\omega)\hat{u}(\omega)$. One immediately observes that the \mathcal{H}_∞ norm defined in (2) is the L^2 -induced operator norm of the underlying convolution operator mapping $u \mapsto y$.

Our goal is to construct another system

$$\mathbf{E}_r \dot{\mathbf{x}}_r(t) = \mathbf{A}_r \mathbf{x}_r(t) + \mathbf{b}_r u(t), \quad y_r(t) = \mathbf{c}_r^T \mathbf{x}_r(t) + d_r u(t) \quad (3)$$

of much smaller order $r \ll n$, with $\mathbf{E}_r, \mathbf{A}_r \in \mathbb{R}^{r \times r}$, $\mathbf{b}_r, \mathbf{c}_r \in \mathbb{R}^r$, and $d_r \in \mathbb{R}$ determined suitably so that in an appropriate sense, y_r approximates y uniformly well over all $u \in L^2(\mathbb{R}^+)$.

Define a *reduced transfer function* associated with (3) as $H_r(s) = \mathbf{c}_r^T (s\mathbf{E}_r - \mathbf{A}_r)^{-1} \mathbf{b}_r + d_r$. Then, for any $u \in L^2(\mathbb{R}^+)$,

$$\|y - y_r\|_{L^2} \leq \|H - H_r\|_{\mathcal{H}_\infty} \|u\|_{L^2}. \quad (4)$$

The *error transfer function*, $H(s) - H_r(s)$, may be rewritten as

$$H(s) - H_r(s) = \mathbf{c}^T (s\mathbf{E} - \mathbf{A})^{-1} \mathbf{b} - [\mathbf{c}_r^T (s\mathbf{E}_r - \mathbf{A}_r)^{-1} \mathbf{b}_r + (d_r - d)].$$

If the d -term in the original model is non-zero then this serves to illustrate how a non-zero d -term from the original model can be absorbed into a reduced-order model, allowing us to assume in all that follows, that $d = 0$ in the original model without loss of generality.

In order to ensure that the output error magnitude, $\|y - y_r\|_{L^2}$, is uniformly small over all bounded inputs u , say with $\|u\|_{L^2} \leq 1$, (4) motivates seeking a reduced system, H_r , that makes $\|H - H_r\|_{\mathcal{H}_\infty}$ small. This leads naturally to the *optimal \mathcal{H}_∞ model reduction problem*:

For a given full-order model $H \in \mathcal{H}_\infty^n$, and given reduction order $r < n$, find a reduced model $H_r \in \mathcal{H}_\infty^r$, that solves

$$\min_{\hat{H}_r \in \mathcal{H}_\infty^r} \|H - \hat{H}_r\|_{\mathcal{H}_\infty}. \quad (5)$$

This problem is an active area of research [2]. We want to develop a methodology that would apply effectively in large-scale settings where, for example, the original state-space dimension, n , could reach or exceed the hundreds of thousands and the reduction order, r , might need to range as high as 200–300 in order to yield reduced-order models with adequate fidelity. Most methods known to us (with the notable exception of balanced truncation, as mentioned below), will be intractable even for modest system order, say, on the order of a few thousand.

A conceptual solution to the optimal \mathcal{H}_∞ problem was given in [26] showing that (5) can be converted into an optimal Hankel norm approximation problem for a special imbedded system with augmented input and output mappings. Unfortunately, the method of [26] is infeasible in practice since it assumes knowledge both of the minimum of (5) as well as a way of constructing the imbedded system. As noted in [26], this information is available (or computationally accessible) only in very special cases.

Several LMI based methods have been presented to solve (5); see, for example, [15, 24, 25, 23, 41] and references therein. These approaches rapidly become computationally intractable with increasing state space dimension. Indeed, the computational examples illustrating the LMI-based methods presented in [15, 24, 25, 23, 41] all had order less than $n = 10$.

The most commonly used methods for obtaining satisfactory \mathcal{H}_∞ reduced models are Gramian-based methods such as *balanced truncation* (BT) [31, 32] and *optimal Hankel norm approximation methods* (HNA) [14]. Both approaches are known to yield small approximation errors in the \mathcal{H}_∞ norm [19, 1], though neither approach generally is capable of producing a globally optimal \mathcal{H}_∞ approximant solving (5). Even though they remain computationally tractable for modest state space dimension (in contrast to existing LMI-based methods), larger state space dimension presents challenges. HNA requires an all-pass dilation of the full-order model followed by a full eigenvalue decomposition. These dense matrix operations, with complexity growing with $\mathcal{O}(n^3)$, limit the utility of HNA for large state space dimension. Notwithstanding these difficulties, [11] demonstrated the applicability of HNA on dynamical systems having state space dimension of up to $\mathcal{O}(10^4)$, using state-of-the-art numerical techniques coupled with parallel processors on clusters.

The situation for BT is a bit better. BT has been applied to systems of order $\mathcal{O}(10^5)$ by solving the underlying Lyapunov equations *iteratively* using ADI-type algorithms, potentially on cluster computers; see, for example, [20, 38, 33, 10, 35, 22] and references therein.

We describe here a model reduction methodology that can be applied effectively even for very large state space dimension and that yields reduced-order models having typically smaller \mathcal{H}_∞ errors than either BT or HNA and at significantly lower cost. Towards this end, we present a new framework for the \mathcal{H}_∞ approximation problem using interpolatory model reduction. By connecting ideas from interpolatory \mathcal{H}_2 model reduction [21], realization theory [29], and complex Chebyshev approximation [39], we develop a numerically efficient interpolation-based method for \mathcal{H}_∞ -approximation in large-scale settings. The main cost of our approach involves the solution of sparse linear systems. We demonstrate that our approach can yield reduced-order systems having \mathcal{H}_∞ errors which are often half that of BT, and very close to (indeed, sometimes better than) that of HNA. For symmetric systems, our method typically produces reduced-order systems with \mathcal{H}_∞ -errors that are near the theoretical best possible of (5).

The rest of the paper is organized as follows: In §2, we briefly review interpolatory model reduction and related approaches for solving the optimal \mathcal{H}_2 approximation problem. §3 introduces the proposed method and §4 illustrates its effectiveness via several numerical examples.

2 Interpolatory model reduction

Given a dynamical system $H(s)$ and a set of points $\{s_1, s_2, \dots, s_k\} \subset \mathbb{C}$, *interpolatory model reduction* produces a dynamical system $H_r(s)$ such that $H_r(s)$ interpolates $H(s)$ together with a prescribed number of derivatives at the points $\{s_1, s_2, \dots, s_k\}$. Although this is posed as a rational interpolation problem, the construction of a solution may be accomplished with a variety of rational Krylov subspace projection techniques. Rational interpolation via projection was first proposed by Skelton *et al.* [42, 44, 45]. Later, Grimme [16] showed how to construct a reduced-order interpolant, using a method of Ruhe.

Theorem 2.1 (Grimme [16]). *Given $H(s) = \mathbf{c}^T(s\mathbf{E} - \mathbf{A})^{-1}\mathbf{b}$ and two point-sets $\mathcal{S}_1, \mathcal{S}_2 \subset \mathbb{C}$ each containing r distinct points: $\mathcal{S}_1 = \{s_1, \dots, s_r\}$, $\mathcal{S}_2 = \{s_{r+1}, \dots, s_{2r}\}$, let*

$$\mathbf{V}_r = [(\mathbf{s}_1\mathbf{E} - \mathbf{A})^{-1}\mathbf{b} \dots (\mathbf{s}_r\mathbf{E} - \mathbf{A})^{-1}\mathbf{b}] \quad \mathbf{W}_r^T = \begin{bmatrix} \mathbf{c}^T(\mathbf{s}_{r+1}\mathbf{E} - \mathbf{A})^{-1} \\ \vdots \\ \mathbf{c}^T(\mathbf{s}_{2r}\mathbf{E} - \mathbf{A})^{-1} \end{bmatrix}. \quad (6)$$

Define a reduced-order model $H_r^0(s) = \mathbf{c}_r^T(s\mathbf{E}_r - \mathbf{A}_r)^{-1}\mathbf{b}_r$, where $d_r = 0$ and

$$\mathbf{E}_r = \mathbf{W}_r^T \mathbf{E} \mathbf{V}_r, \quad \mathbf{A}_r = \mathbf{W}_r^T \mathbf{A} \mathbf{V}_r, \quad \mathbf{b}_r = \mathbf{W}_r^T \mathbf{b}, \quad \text{and} \quad \mathbf{c}_r^T = \mathbf{c}^T \mathbf{V}_r. \quad (7)$$

Then $H(s_i) = H_r^0(s_i)$, for $i = 1, \dots, 2r$.

If $s_k = s_\ell$, for some $1 \leq k \leq r$ and $r + 1 \leq \ell \leq 2r$, then additionally $H'(s_k) = H_r^{0'}(s_k)$.

Higher-order derivatives can be matched similarly; for details, see [16, 4].

2.1 \mathcal{H}_2 -optimality conditions

Theorem 2.1 gives explicitly computable conditions that will yield a reduced-order model satisfying $2r$ interpolation conditions; one need only solve $2r$ linear algebraic systems to form the columns of \mathbf{V}_r and \mathbf{W}_r . Notably, Theorem 2.1 carries no hint of how best to choose these interpolation points. A method for determining interpolation points that leads to reduced-order models that are (locally) optimal with respect to the \mathcal{H}_2 error was developed in [21] and will be a point of departure for the approach we propose here.

For a SISO dynamical system $H(s)$, the \mathcal{H}_2 norm is defined as

$$\|H\|_{\mathcal{H}_2} = \left(\frac{1}{2\pi} \int_{-\infty}^{\infty} |H(j\omega)|^2 d\omega \right)^{1/2}. \quad (8)$$

Then, for a given full-order model $H(s)$, and selected reduction order $r < n$, the *optimal \mathcal{H}_2 approximation problem* seeks a reduced model, $H_r^0(s)$, that solves

$$\min_{\hat{H}_r^0 \in \mathcal{H}_2^r} \|H - \hat{H}_r^0\|_{\mathcal{H}_2}. \quad (9)$$

The approximation problem (9) has been studied extensively; see, for example, [30],[43],[21], [36], [40], [18], [6], [7],[47] and references therein. First-order necessary conditions for \mathcal{H}_2 -optimal approximation may be formulated in terms of interpolation conditions:

Theorem 2.2 ([30, 21]). *Given a full-order model $H(s)$, let $H_r^0(s)$ be an \mathcal{H}_2 -optimal reduced order model of order r , with simple poles $\hat{\lambda}_1, \dots, \hat{\lambda}_r$. Then,*

$$H(-\hat{\lambda}_i) = H_r^0(-\hat{\lambda}_i) \quad \text{and} \quad H'(-\hat{\lambda}_i) = H_r^{0'}(-\hat{\lambda}_i) \quad \text{for} \quad i = 1, \dots, r, \quad (10)$$

where $'$ denotes differentiation with respect to the frequency parameter, s .

These necessary conditions characterize the \mathcal{H}_2 -optimal reduced order model as a rational Hermite interpolant matching the full-order transfer function and its derivative at mirror images of the reduced-order system poles. This can be accomplished with the help of Theorem 2.1 once the poles of $H_r^0(s)$ are known. Of course, the poles of $H_r^0(s)$ are not known *a priori*, but they can be computed iteratively using the *Iterative Rational Krylov Algorithm* (IRKA) developed by Gugercin *et al.* [21].

Algorithm IRKA. *Iterative Rational Krylov Algorithm [21]*

Given a full-order $H(s)$, a reduction order r , and convergence tolerance tol .

1. Make an initial selection of interpolation points s_i , for $i = 1, \dots, r$ that is closed under complex conjugation.
2. Construct \mathbf{V}_r and \mathbf{W}_r as in (6) with $s_{i+r} = s_i$ for $i = 1, \dots, r$
3. while (relative change in $\{s_i\} < \text{tol}$)
 - a) $\mathbf{E}_r = \mathbf{W}_r^T \mathbf{E} \mathbf{V}_r$ and $\mathbf{A}_r = \mathbf{W}_r^T \mathbf{A} \mathbf{V}_r$
 - b) Solve $r \times r$ eigenvalue problem $\mathbf{A}_r \mathbf{u} = \lambda \mathbf{E}_r \mathbf{u}$.
 - c) Assign $s_i = s_{i+r} \leftarrow -\lambda_i(\mathbf{A}_r, \mathbf{E}_r)$ for $i = 1, \dots, r$.
 - d) Update \mathbf{V}_r and \mathbf{W}_r as in (6) using new $\{s_i\}$.
4. $\mathbf{E}_r = \mathbf{W}_r^T \mathbf{E} \mathbf{V}_r$, $\mathbf{A}_r = \mathbf{W}_r^T \mathbf{A} \mathbf{V}_r$, $\mathbf{b}_r = \mathbf{W}_r^T \mathbf{b}$, $\mathbf{c}_r^T = \mathbf{c}^T \mathbf{V}_r$, and $d_r = 0$.

IRKA is a fixed point iteration that in the SISO case typically exhibits rapid convergence to a local minimizer of the \mathcal{H}_2 -optimal model reduction problem. Sparsity in \mathbf{E} and \mathbf{A} can be well-exploited in the linear solves of Steps 2 and 3c and IRKA has been remarkably successful in producing high fidelity reduced-order approximations in large-scale settings; it has been applied successfully in finding \mathcal{H}_2 -optimal reduced models for systems of high order (e.g., $n > 160,000$, see [27]). For details on the algorithm, we refer to the original source [21].

3 An interpolatory approach for \mathcal{H}_∞ approximation

The principal result that defines the character of our approach is an analog to the Chebyshev Equioscillation Theorem provided by Trefethen in [39]. We restate this below using terminology from the present context.

Theorem 3.1 (Trefethen [39]). *Suppose $H(s)$ is a transfer function associated with a dynamical system as in (1). Let $H_r^{\text{opt}}(s)$ be an optimal \mathcal{H}_∞ approximation to $H(s)$ (i.e., a solution to (5)) and let $H_r(s)$ be any r^{th} order stable approximation to $H(s)$ that interpolates $H(s)$ at $2r + 1$ points in the open right half plane. Then*

$$\min_{\omega \in \mathbb{R}} |H(j\omega) - H_r(j\omega)| \leq \|H - H_r^{\text{opt}}\|_{\mathcal{H}_\infty} \leq \|H - H_r\|_{\mathcal{H}_\infty}$$

In particular, if $|H(j\omega) - H_r(j\omega)| = \text{const}$ for all $\omega \in \mathbb{R}$ then $H_r(s)$ is itself an optimal \mathcal{H}_∞ approximation to $H(s)$.

One sees from this that a good \mathcal{H}_∞ approximation will be obtained when the modulus of the error, $|H(s) - H_r(s)|$, is nearly constant as $s = j\omega$ runs along the imaginary axis, and so we aim to select $2r + 1$ interpolation points in the open right half plane that will induce this. By utilizing Theorem 2.1, we may locate $2r$ interpolation points in the right half plane as we like, producing an interpolating reduced-order system, $H_r^0(s)$. Also, $H(\infty) = H_r^0(\infty) = 0$ so we can exploit the freedom in choosing d_r to move the $(2r + 1)^{\text{st}}$ interpolation point from ∞ into the open right half-plane. Note that the straightforward construction, $H_r(s, d_r) = H_r^0(s) + d_r$, creates a reduced-order model that has *all* interpolation points depending on d_r . We prefer a different formulation that uncouples the $2r$ interpolation points associated with $H_r^0(s)$ from the influence of d_r . The construction that accomplishes this was introduced in [29] (see also [5] for a formulation close to what we use here).

Theorem 3.2. *Given $H(s) = \mathbf{c}^T(s\mathbf{I} - \mathbf{A})^{-1}\mathbf{b}$ and two point-sets $\mathcal{S}_1, \mathcal{S}_2 \subset \mathbb{C}$ each containing r distinct points: $\mathcal{S}_1 = \{s_1, \dots, s_r\}$, $\mathcal{S}_2 = \{s_{r+1}, \dots, s_{2r}\}$, let $\mathbf{V}_r, \mathbf{W}_r, \mathbf{E}_r, \mathbf{A}_r, \mathbf{b}_r$, and \mathbf{c}_r be as defined in Theorem 2.1. For any given $d_r \in \mathbb{R}$, define a new reduced-order system*

$$H_r(s, d_r) = (\mathbf{c}_r - d_r \mathbf{e})^T (s\mathbf{E}_r - \mathbf{A}_r - d_r \mathbf{e} \mathbf{e}^T)^{-1} (\mathbf{b}_r - d_r \mathbf{e}) + d_r \quad (11)$$

where \mathbf{e} denotes a vector of ones. Define auxiliary reduced systems:

$$\begin{aligned} H_r^0(s) &= \mathbf{c}_r^T (s\mathbf{E}_r - \mathbf{A}_r)^{-1} \mathbf{b}_r, & G_1(s) &= \mathbf{e}^T (s\mathbf{E}_r - \mathbf{A}_r)^{-1} \mathbf{b}_r, \\ G_2(s) &= \mathbf{c}_r^T (s\mathbf{E}_r - \mathbf{A}_r)^{-1} \mathbf{e}, & \text{and} & & G_3(s) &= \mathbf{e}^T (s\mathbf{E}_r - \mathbf{A}_r)^{-1} \mathbf{e}. \end{aligned}$$

Then

$$H_r(s, d_r) = H_r^0(s) + d_r \frac{(G_1(s) - 1)(G_2(s) - 1)}{1 - d_r G_3(s)} \quad (12)$$

and for all $d_r \in \mathbb{R}$

- $H(s_i) = H_r^0(s_i) = H_r(s_i, d_r)$, for $i = 1, \dots, 2r$.
- if $\mathcal{S}_1 \equiv \mathcal{S}_2$ then $H'(s_i) = H_r^{0'}(s_i) = H_r'(s_i, d_r)$ for $i = 1, \dots, r$,

where $'$ denotes the derivative with respect to the frequency parameter, s .

PROOF: The expression (12) follows from (11) with straightforward manipulations that begin with the Sherman-Morrison formula:

$$(s\mathbf{E}_r - \mathbf{A}_r - d_r \mathbf{e} \mathbf{e}^T)^{-1} = (s\mathbf{E}_r - \mathbf{A}_r)^{-1} + \frac{d_r}{1 - d_r G_3(s)} (s\mathbf{E}_r - \mathbf{A}_r)^{-1} \mathbf{e} \mathbf{e}^T (s\mathbf{E}_r - \mathbf{A}_r)^{-1}$$

Define $\mathbf{P}(s) = \mathbf{V}_r (s\mathbf{E}_r - \mathbf{A}_r)^{-1} \mathbf{W}_r^T (s\mathbf{E} - \mathbf{A})$. Observe that $\mathbf{P}(s)$ is a (skew) projection onto $\text{Ran}(\mathbf{V}_r)$ for any $s \in \mathbb{C}$ for which it is well-defined and so we have

$$\begin{aligned} \mathbf{V}_r \mathbf{e}_k &= \mathbf{P}(s_k) \mathbf{V}_r \mathbf{e}_k = [\mathbf{V}_r (s_k \mathbf{E}_r - \mathbf{A}_r)^{-1} \mathbf{W}_r^T (s_k \mathbf{E} - \mathbf{A})] (s_k \mathbf{E} - \mathbf{A})^{-1} \mathbf{b} \\ &= \mathbf{V}_r (s_k \mathbf{E}_r - \mathbf{A}_r)^{-1} \mathbf{W}_r^T \mathbf{b} = \mathbf{V}_r (s_k \mathbf{E}_r - \mathbf{A}_r)^{-1} \mathbf{b}_r \end{aligned}$$

Linear independence of the columns of \mathbf{V}_r then implies $\mathbf{e}_k = (s_k \mathbf{E}_r - \mathbf{A}_r)^{-1} \mathbf{b}_r$ and as a consequence, $G_1(s_k) = 1$, for $k = 1, 2, \dots, r$. A similar argument yields $G_2(s_\ell) = 1$, for $\ell = r+1, r+2, \dots, 2r$. Taken together, we get that $H_r^0(s_i) = H_r(s_i, d_r)$ for $i = 1, 2, \dots, 2r$ and if $\mathcal{S}_1 \equiv \mathcal{S}_2$ then $(G_1(s) - 1)(G_2(s) - 1) = \prod_{i=1}^r (s - s_i)^2$ so that $H_r^{0'}(s_i) = H_r'(s_i, d_r)$ as well. \square

Let $\{H_r(s, \cdot)\}_{d_r}$ denote the set of all transfer functions $H_r(s, d_r)$ with d_r ranging over \mathbb{R} . The freedom we have in choosing d_r is significant to us for at two reasons. First, $\{H_r(s, \cdot)\}_{d_r}$ is a parameterization of the set of all proper rational functions of degree r having real coefficients that satisfy the same interpolation constraints as $H_r^0(s)$ (see e.g., [29]). Second, it is now possible to construct reduced-order models of order r satisfying $2r+1$ interpolation conditions, which is an essential step towards constructing reduced-order models that are optimal in the \mathcal{H}_∞ -norm. Since $H_r(s, d_r)$ interpolates $H(s)$ at s_1, \dots, s_{2r} for any d_r , one could select an additional (real) interpolation point, $s_{2r+1} > 0$ and directly calculate from (12) the value of d_r that enforces $H_r(s_{2r+1}, d_r) = H(s_{2r+1})$:

$$d_r = \frac{H(s_{2r+1}) - H_r^0(s_{2r+1})}{(G_1(s_{2r+1}) - 1)(G_2(s_{2r+1}) - 1) + G_3(s_{2r+1})(H(s_{2r+1}) - H_r^0(s_{2r+1}))}.$$

We avoid the necessity of explicitly selecting s_{2r+1} . Instead, as discussed below, d_r will be chosen directly to decrease the \mathcal{H}_∞ error.

3.1 An algorithm for \mathcal{H}_∞ approximation

It has been observed (e.g., see [21],[4]) that \mathcal{H}_2 optimal interpolation points produced by IRKA yield reduced-order models that are frequently high-fidelity \mathcal{H}_∞ approximations to the original system as well as being (locally) \mathcal{H}_2 -optimal. Indeed, it is usual that these \mathcal{H}_2 -optimal models produce \mathcal{H}_∞ error norms that are comparable to that of balanced truncation and sometimes are better. Therefore, we begin by applying **Algorithm IRKA** to obtain $2r$ interpolation points that determine an \mathcal{H}_2 -optimal reduced model, $H_r^0(s)$. This choice for $H_r^0(s)$ defines a family of approximations parameterized by d_r , $\{H_r(s, \cdot)\}_{d_r}$. We proceed by (approximately) minimizing the \mathcal{H}_∞ error with respect to d_r . This is a summary of **Algorithm IHA** below.

Our justification for this approach is simple. The \mathcal{H}_2 optimal approximation yields an interpolation point distribution which performs ideally in an \mathcal{H}_∞ norm approximation setting. We therefore preserve this distribution of interpolation points using **Theorem 3.2** and vary the d_r parameter in such a way as to drive down the \mathcal{H}_∞ error - centering the error curve about the origin in the process. $H_r^*(s)$ will denote an \mathcal{H}_∞ approximant having 1) an \mathcal{H}_2 optimal pole distribution (from Step 1 of **Algorithm IHA**) and 2) an optimally chosen d_r^* (from Step 2).

Algorithm IHA. *Interpolatory \mathcal{H}_∞ Approximation:*

Given a full-order model, $H(s)$, and a reduction order, r .

1. Apply Algorithm IRKA to compute $2r$ \mathcal{H}_2 -optimal interpolation points and an associated \mathcal{H}_2 -optimal reduced model, $H_r^0(s)$.
2. Find $d_r^* = \arg \min_{d_r \in \mathbb{R}} \|H - H_r\|_{\mathcal{H}_\infty}$ where $H_r = H_r(s, d_r)$ is defined in (12).
3. Construct the final \mathcal{H}_∞ approximant as $H_r^*(s) = H_r(s, d_r^*)$.

3.2 Efficient Implementation of Step 2 of Algorithm IHA

The major contributions to the cost of IHA come from linear solves arising in Step 1 (from IRKA) and the \mathcal{H}_∞ norm evaluations required in solving the (scalar) nonlinear optimization problem in Step 2. \mathcal{H}_∞ norm evaluation involves repeated solution of several large-scale Riccati equations of order $n + r$. Note that solving even a single Riccati equation, let alone several of them, will be a formidable task for n on the scale of tens of thousands or larger, which is the range of system dimension of interest here. We describe below an effective strategy to circumvent this difficulty.

The optimization problem of Step 2 can be rewritten (from Theorem 3.2) as

$$\min_{d_r \in \mathbb{R}} \left\| H(s) - H_r^0(s) - \frac{d_r(G_1(s) - 1)(G_2(s) - 1)}{1 - d_r G_3(s)} \right\|_{\mathcal{H}_\infty}$$

where $H_r^0(s)$ is a reduced-model obtained by IRKA in Step 1 of Algorithm IHA.

If one can find a reduced-order approximation, $F_k(s)$, to the error system, $H(s) - H_r^0(s)$, with modest fidelity and order $k \ll n$, then an optimal d_r -term could be accurately approximated by solving a much simpler (surrogate) optimization problem

$$\min_{d_r \in \mathbb{R}} \left\| F_k(s) - \frac{d_r(G_1(s) - 1)(G_2(s) - 1)}{1 - d_r G_3(s)} \right\|_{\mathcal{H}_\infty} \quad (13)$$

Provided $k \ll n$, the cost of solving (13) will be negligible compared to that of original problem. Of course, whatever advantage this strategy may bring could be nullified if the cost of obtaining $F_k(s)$ is significant. By using a Loewner matrix approach developed by Mayo and Antoulas [29] and described briefly below, we are able to obtain $F_k(s)$ at negligible cost relative to the computational demands already incurred in Step 1. Indeed, we reuse information obtained in the course of IRKA in Step 1 to obtain for negligible additional effort, a reduced error model $F_k(s)$ having modest fidelity, which is adequate for the demands of Step 2.

The Loewner matrix approach as developed by Mayo and Antoulas [29] permits “data-driven” model reduction; one need not have access to state-space matrices determining a

realization of the full order system. Only “response measurements” are used, that is, transfer function evaluations. Reduced-order models will be constructed directly that interpolate this “measured data”.

Given a full order dynamical system, $F(s)$ (eventually we will take $F(s) = H(s) - H_r^0(s)$), assume that we have evaluated $F(s)$ and $F'(s)$ at a set of distinct points $\{s_1, s_2, \dots, s_\ell\} \subset \mathbb{C}$. We consider how to construct a system $F_k(s) = \hat{\mathbf{c}}_k^T (s\hat{\mathbf{E}}_k - \hat{\mathbf{A}}_k)^{-1} \hat{\mathbf{b}}_k$ from this data so that

$$F(s_i) = F_k(s_i) \text{ and } F'(s_i) = F'_k(s_i) \text{ for } i = 1, 2, \dots, \ell.$$

Define matrices $\mathbb{L} \in \mathbb{C}^{\ell \times \ell}$ and $\mathbb{M} \in \mathbb{C}^{\ell \times \ell}$ as

$$(\mathbb{L})_{i,j} := \begin{cases} \frac{F(s_i) - F(s_j)}{s_i - s_j} & \text{if } i \neq j \\ F'(s_i) & \text{if } i = j \end{cases} \quad (\mathbb{M})_{i,j} := \begin{cases} \frac{s_i F(s_i) - s_j F(s_j)}{s_i - s_j} & \text{if } i \neq j \\ [sF(s)]'|_{s=s_i} & \text{if } i = j \end{cases} \quad (14)$$

\mathbb{L} is the *Loewner matrix* associated with interpolation points s_1, s_2, \dots, s_ℓ and the dynamical system $F(s)$; \mathbb{M} is the corresponding *shifted Loewner matrix* (see [29] for details). Once, \mathbb{L} and \mathbb{M} are constructed, a rational Hermite interpolant may be constructed as follows.

Choose k so that

$$\text{rank}(s_i \mathbb{L} - \mathbb{M}) = \text{rank}[\mathbb{L} \ \mathbb{M}] = \text{rank} \begin{bmatrix} \mathbb{L} \\ \mathbb{M} \end{bmatrix} \geq k, \text{ for } i = 1, 2, \dots, \ell.$$

Let $s_i \mathbb{L} - \mathbb{M} = \mathbf{Y} \boldsymbol{\Theta} \mathbf{X}^*$, be the SVD of $s_i \mathbb{L} - \mathbb{M}$ for some choice of $1 \leq i \leq \ell$. Let $\mathbf{Y}_k \in \mathbb{C}^{\ell \times k}$ and $\mathbf{X}_k \in \mathbb{C}^{\ell \times k}$ be the leading k columns of \mathbf{Y} and \mathbf{X} , respectively (associated with a truncated SVD of order k). Then, $F_k(s) = \hat{\mathbf{c}}_k^T (s\hat{\mathbf{E}}_k - \hat{\mathbf{A}}_k)^{-1} \hat{\mathbf{b}}_k$ is defined via

$$\hat{\mathbf{E}}_k = -\mathbf{Y}_k^* \mathbb{L} \mathbf{X}_k, \quad \hat{\mathbf{A}}_k = -\mathbf{Y}_k^* \mathbb{M} \mathbf{X}_k, \quad \hat{\mathbf{b}}_k = \mathbf{Y}_k^* \mathbf{Z}, \quad \hat{\mathbf{c}}_k = \mathbf{Z}^T \mathbf{X}_k,$$

where $\mathbf{Z} = [F(s_1), F(s_2), \dots, F(s_\ell)]^T$. One may consider k as a truncation index bounded by $\text{rank}(s_i \mathbb{L} - \mathbb{M}) \leq \ell$. Depending on whether k is chosen to be equal to $\text{rank}(s_i \mathbb{L} - \mathbb{M})$ or smaller, $F_k(s)$ will be either an exact or an approximate interpolant, respectively. In practice, one should choose k no larger than the numerical rank of $s_i \mathbb{L} - \mathbb{M}$, which can be determined by a Singular Value Decomposition (SVD) of $s_i \mathbb{L} - \mathbb{M}$. See [29] for a full development of these ideas.

Now let us consider how this approach fits into our framework for approximating $F(s) = H(s) - H_r^0(s)$. Until convergence occurs within Step 1 of Algorithm IHA, every cycle of Step 3 in Algorithm IRKA provides a sampling of $H(s)$ and $H'(s)$ at r interpolation points – generally a different set of interpolation points in each cycle. (Recall that Step 3 of Algorithm IRKA constructs a Hermite interpolant at a current set of r interpolation points.) Assume that Algorithm IRKA takes q steps to convergence. When Step 1 of Algorithm IHA concludes, we will have had $H(s)$ and $H'(s)$ sampled at a total of $\ell = q \times r$ interpolation points.

We collect these interpolation points and transfer function evaluations throughout IRKA. Once IRKA converges, (yielding an \mathcal{H}_2 -optimal model, $H_r^0(s)$), we evaluate H_r^0 and $H_r^{0'}$ at these ℓ points as well. Since the order of $H_r^0(s)$ is r , the cost of these function evaluations is negligible. After the completion of Step 1 of Algorithm IHA, we have an ℓ -fold sampling of $F(s) = H(s) - H_r^0(s)$ and $F'(s)$ with virtually no additional computational cost beyond what was needed for Step 1 itself. Then, we simply apply the Loewner matrix approach described above to construct $F_k(s)$. The choice of k will be clarified via numerical examples in §4.

Note that once Step 1 of Algorithm IHA is completed, the remaining part of Algorithm IHA incurs negligible additional computational cost dominated typically by the cost of an $\ell \times \ell$ SVD computation with $\ell = q \times r$. Since IRKA typically converges rather fast, and especially in the SISO case focused on here, ℓ is invariably modest in size. In all of our numerical examples, we have never needed to compute an SVD of size larger than 200×200 ; a trivial computation. Moreover, in all of our numerical examples, k never exceeded 33; hence making the solution of the optimization problem in Step 2 quite cheap.

4 Numerical Experiments

In this section we illustrate the performance of IHA on various benchmark models for model reduction and compare its performance with that of BT and HNA. We note that unlike our approach, the generic BT will yield $d_r = 0$. Therefore, in order to present a fair comparison to BT, we vary the d_r term in BT as well and use the d_r -term yielding the minimum \mathcal{H}_∞ norm. We will use the term “modified balanced truncation” (or MBT) to refer to BT with an optimally chosen d_r term.

4.1 PEEC Model

The full-order system is the spiral inductor system PEEC model [12] of order $n = 1434$. The system is state-space-symmetric (SSS), i.e. the transfer function $H(s) = \mathbf{c}^T(s\mathbf{E} - \mathbf{A})^{-1}\mathbf{b}$ satisfies $\mathbf{E} = \mathbf{E}^T > 0$, $\mathbf{A} = \mathbf{A}^T$ and $\mathbf{c} = \mathbf{b}$. SSS systems appear in many important applications such as in the analysis of RC circuits, and has been the subject of several model reduction papers; e.g, see [28, 37, 34, 46]. We first illustrate the effect of the d_r -term modification for MBT and for the proposed method as in Step 2 of Algorithm IHA. In MBT, once BT is performed, we vary the d_r -term and measure the resulting \mathcal{H}_∞ error norm for each d_r . In IHA, once IRKA is performed, we vary the d_r term together with appropriate modification to A_r , b_r and c_r as in Theorem 3.2 and once again measure the resulting \mathcal{H}_∞ error norm for each d_r . We note that this is for illustration purposes only and is not the way IHA computes the optimal d_r -term. IHA finds the optimal d_r in a numerically effective way as outlined in §3.2. The results are shown in Figure 1 for $r = 2$. As the figure shows,

while there is essentially no gain in MBT from changing the d_r -term, for our method the error is reduced by a factor larger than two. Even though the starting point $d_r = 0$ has a higher \mathcal{H}_∞ -error for the \mathcal{H}_2 -optimal approximation than BT, by the d_r -term optimization, the proposed method reduces the error to a value significantly lower than that of MBT with essentially negligible computational cost.

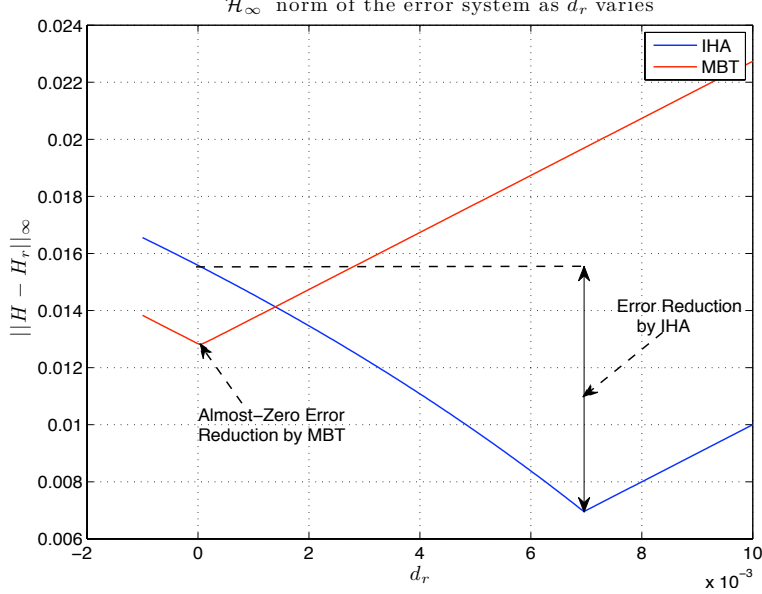


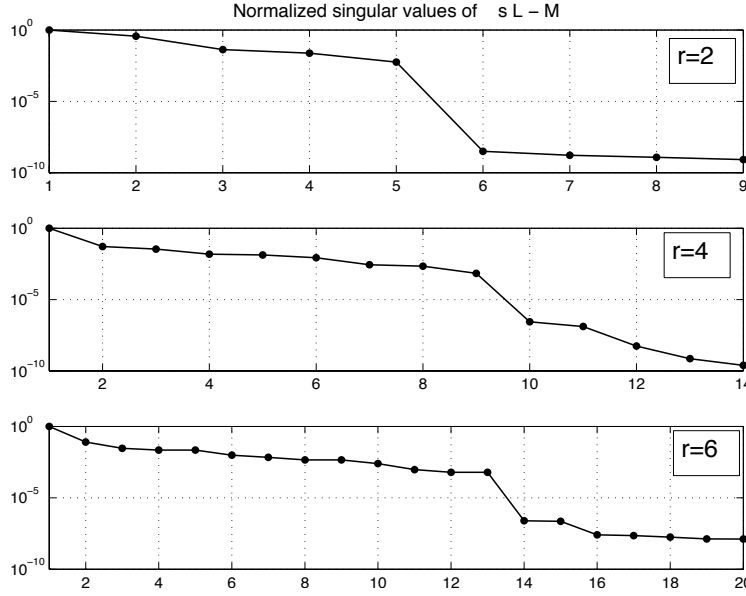
Figure 1: Comparison of the \mathcal{H}_∞ Error as the d_r -term varies for IHA and MBT

Before presenting the comparisons between IHA, MBT, and HNA, we illustrate the efficiency of the methodology outlined in §3.2 in solving the optimization problem in Algorithm IHA; in other words in finding the optimal d_r -term in Figure 1. For the three r values $r = 2, 4, 6$, we implement IHA both by exactly solving Step 2 and by the method of §3.2. Table 1 tabulates the results where the resulting optimal d_r values and the \mathcal{H}_∞ error norms for both methods together with the order- k used in method of §3.2 are listed. As the table clearly illustrates that the Loewner matrix approach yields d_r terms and the \mathcal{H}_∞ error norms which are very close to true-optimal values of the underlying optimization problem in Step 2 of Algorithm IHA. More importantly, this is achieved with negligible computational cost where the function evaluations are the \mathcal{H}_∞ norm computations for an order k system only as opposed to order $n + r$. One pattern we have observed via several SSS models is that $k = 2r + 1$ is a natural choice. This pattern repeated itself for every SSS example we have tried. There was a clear cut-off point in the singular values of the matrix $s_i\mathbb{L} - \mathbb{M}$ at $(2r + 1)^{\text{th}}$ singular value. The decay of these singular for all three r values are shown in Figure 2 supporting the $k = 2r + 1$ choice.

Next, to compare IHA, MBT, and HNA, we reduce the order of the system to $r = 2, 4, 6$. The resulting relative \mathcal{H}_∞ error values together with the lower bound (i.e. $\sigma_{r+1}/\|H\|_{\mathcal{H}_\infty}$

Table 1: Solution of the optimization problem in Step 2

r	Exact		Loewner		
	d_r^*	$\ H - H_r^*\ _{\mathcal{H}_\infty}$	d_r^*	$\ H - H_r^*\ _{\mathcal{H}_\infty}$	k
2	6.9577×10^{-3}	4.4522×10^{-3}	6.9659×10^{-3}	4.4574×10^{-3}	5
4	1.0041×10^{-4}	8.6577×10^{-5}	1.0076×10^{-4}	8.7114×10^{-5}	9
6	2.7795×10^{-6}	4.4771×10^{-6}	2.7804×10^{-6}	4.4857×10^{-6}	13


 Figure 2: The decay of the singular values of $s_i \mathbb{L} - \mathbb{M}$ for PEEC Model

where σ_{r+1} denotes the $(r+1)^{\text{th}}$ Hankel singular value of $H(s)$ are listed in Table 2. The lowest error value for each r is shown in bold font. For every r , IHA outperforms MBT by almost a factor of two. Also it performs very close to HNA, indeed outperforms it for $r = 4$. This shows the strength of the proposed method. Without solving any Lyapunov equations and without the need for any large-scale \mathcal{H}_∞ norm computation, our methods consistently outperforms BT by a significant amount and performs as nearly as and sometimes better than HNA. We also note that \mathcal{H}_∞ error values for IHA is very close to the lower bound given by $\sigma_{r+1}/\|H\|_{\mathcal{H}_\infty}$. We can relate this to Theorem 3.1. As desired by Theorem 3.1, for each order of approximation shown in Table 2, the reduced-model due to IHA results in exactly $2r + 1$ interpolation points in the right-half plane and a nearly circular error curve as illustrated in Figure 3. $2r$ of these zeros result from IRKA; indeed these are r distinct zeroes with multiplicity 2. Then, the $(2r + 1)^{\text{th}}$ zero is obtained by introducing the d_r term. For example, for the case $r = 6$, computing the optimal d_r -term in turn placed an additional zero at the point 6.60×10^8 .

Table 2: Relative \mathcal{H}_∞ error norms for the PEEC Model

r	IHA	MBT	HNA	Lower bound
2	4.45×10^{-3}	8.21×10^{-3}	3.95×10^{-3}	3.72×10^{-3}
4	8.66×10^{-5}	2.78×10^{-4}	1.24×10^{-4}	7.79×10^{-5}
6	4.48×10^{-6}	8.16×10^{-6}	3.41×10^{-6}	3.15×10^{-6}

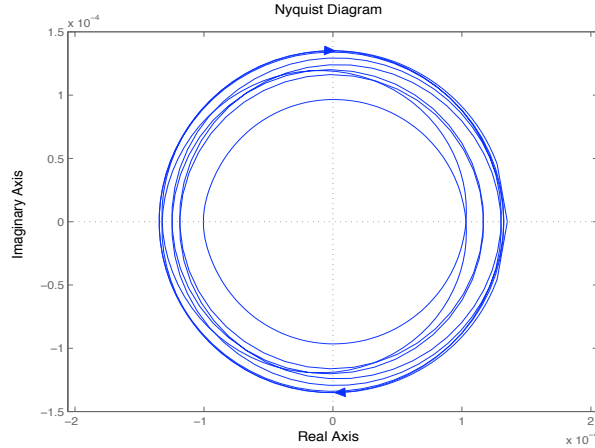


Figure 3: The Nyquist plot of the error system $H - H_r^*$ for PEEC Model

We want to note that the findings in this SSS example are common to all other SSS examples we have tried. The \mathcal{H}_∞ error due to IHA have been always around half of MBT, and $k = 2r+1$ has been the clear cut-off point in the Loewner matrix approach. Due to the page limitations, we omit these examples. For some other SSS examples, we refer the reader to [13].

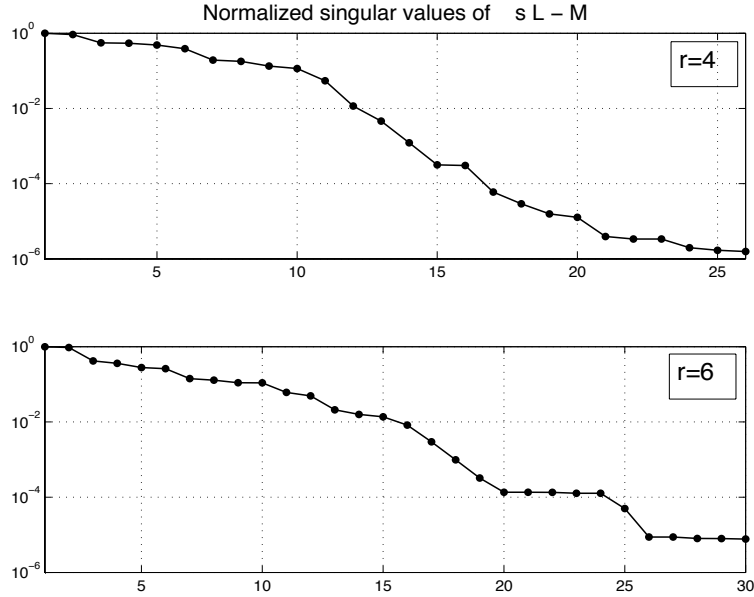
4.2 CD Player Model

Next, we demonstrate the proposed method on the CD player model of order $n = 120$. For details on this model, see [3, 12]. We reduce the order to $r = 2, 4, 6, 8, 10$ using IHA; stopping at $r = 10$ as the relative error fell below 10^{-3} . As done in the previous example, we illustrate the effect of solving the optimization problem in Step 2 of Algorithm IHA exactly and by the method of §3.2. The results are listed in Table 3. As in the previous case, the Loewner matrix approach yields the \mathcal{H}_∞ error norms which are very close to true-optimal values of the underlying optimization problem. Once again, the function evaluations are much simpler as k never exceeds 33. In this example, we chose the value of k as the normalized singular values of $s_i\mathbb{L} - \mathbb{M}$ drops below the tolerance of 10^{-5} . Figure 4 shows this decay behavior for $r = 4$ and $r = 6$.

Next, we compare IHA with MBT and HNA. The results are illustrated in Table 4 where the

Table 3: Solution of the optimization problem in Step 2

r	Exact		Loewner		
	d_r^*	$\ H - H_r^*\ _{\mathcal{H}_\infty}$	d_r^*	$\ H - H_r^*\ _{\mathcal{H}_\infty}$	k
2	-3.6728	3.6597×10^{-1}	-3.6545	3.6604×10^{-1}	2
4	3.5019×10^{-1}	2.1318×10^{-2}	2.4819×10^{-1}	2.1422×10^{-2}	20
6	2.9538×10^{-1}	1.0155×10^{-2}	2.0763×10^{-1}	1.0426×10^{-2}	25
8	1.3888×10^{-1}	4.8357×10^{-3}	1.3625×10^{-1}	4.8526×10^{-3}	32
10	-3.5750×10^{-2}	8.5384×10^{-4}	-3.2438×10^{-2}	8.9952×10^{-4}	33


 Figure 4: The decay of the singular values of $s_i L - M$ for the CD Player Model

minumum value for each r is shown in bold font. The first observation is that for every r value, the proposed approach outperforms MBT. Moreover, except for the $r = 2$ and $r = 4$ cases, IHA outperforms HNA as well.

Before moving to the next example, we illustrate the effect of the d_r -term modification in our proposed method as opposed to MBT. In Figure 5, we show how the *absolute* \mathcal{H}_∞ -error changes as we vary the d_r -term both in IHA and in MBT for $r = 10$. Note that for both cases $d_r = 0$ is the starting point. While the \mathcal{H}_∞ -error reduces marginally from 0.0905 to 0.0852 in MBT—only a 5.86% reduction, the gain is much more significant in IHA where we reduce the \mathcal{H}_∞ -error from 0.0938 down to 0.0585, a significant 37.67% reduction in the \mathcal{H}_∞ error. Even though the starting point $d_r = 0$ has a higher \mathcal{H}_∞ -error for the \mathcal{H}_2 -optimal approximation than BT, by the effective d_r -term optimization, the proposed method reduces the error to a value significantly lower than that of MBT.

Table 4: Relative \mathcal{H}_∞ -norm Error norms for the CD Player Model

r	IHA	MBT	HNA
2	3.66×10^{-1}	3.68×10^{-1}	3.35×10^{-1}
4	2.14×10^{-2}	2.25×10^{-2}	2.00×10^{-2}
6	1.04×10^{-2}	1.19×10^{-2}	1.23×10^{-2}
8	4.85×10^{-3}	6.40×10^{-3}	5.99×10^{-3}
10	8.99×10^{-4}	1.24×10^{-3}	1.08×10^{-3}

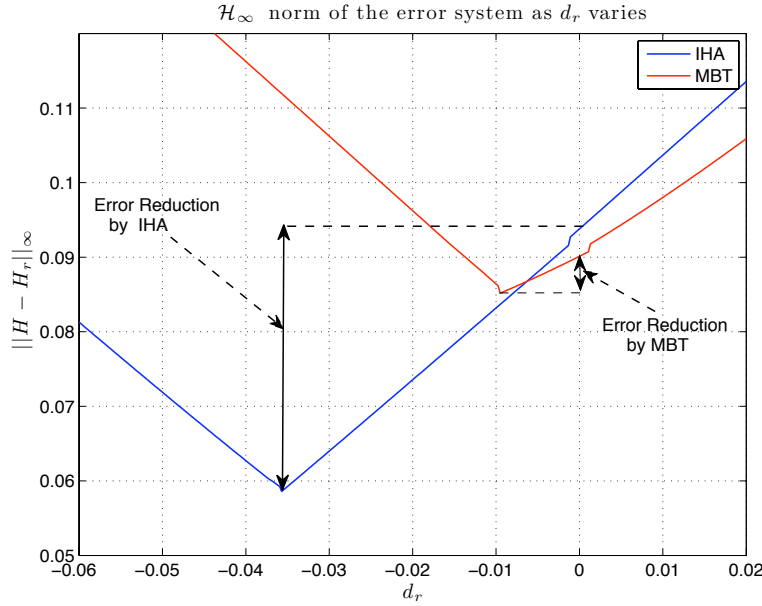


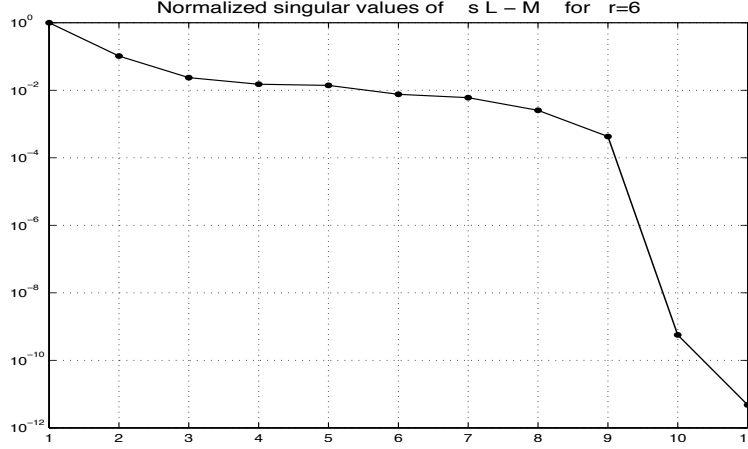
Figure 5: \mathcal{H}_∞ error as a function of the d_r -term in MBT and IHA

4.3 Heat Model

The full-order model is a plate with two heat sources and two points of measurements, and described by the heat equation as explained in [3, 17]. A model of order $n = 197$ is obtained by spatial discretization. We choose a SISO subsystem corresponding to the first input and first output. Using IHA, we reduce the order to $r = 2, 4$ and $r = 6$. As in the previous examples, we first tabulate, in Table 5, the results for solving the Step 2 of Algorithm IHA exactly and by the method of §3.2. The conclusion is the same as before: The Loewner matrix approach yields the \mathcal{H}_∞ error norms and optimal- d_r values which are very close to the true-optimal values of the underlying optimization problem in Step 2 of Algorithm IHA, indeed exact to the fifth digit for the $r = 6$ case. The decay of the singular values of $s_i\mathbb{L} - \mathbb{M}$ is shown in Figure 6, illustrating the choice of k . Only the $r = 6$ case is presented; the other cases show the same pattern.

Table 5: Solution of the optimization problem in Step 2

r	Exact		Loewner		
	d_r^*	$\ H - H_r^*\ _{\mathcal{H}_\infty}$	d_r^*	$\ H - H_r^*\ _{\mathcal{H}_\infty}$	k
2	-2.0694×10^{-1}	1.0710×10^{-2}	-2.0700×10^{-1}	1.0711×10^{-2}	7
4	2.0875×10^{-2}	8.9082×10^{-4}	2.0813×10^{-2}	8.9166×10^{-4}	9
6	-5.6250×10^{-4}	2.3578×10^{-5}	-5.6250×10^{-1}	2.3578×10^{-5}	13


 Figure 6: The decay of the singular values of $s_i \mathbb{L} - \mathbb{M}$ for the Heat Model

Results for comparison with MBT and HNA are shown in Table 6. Once more, the proposed method consistently yields better \mathcal{H}_∞ performance than MBT. Even though for $r = 2$ the proposed method leads to smaller \mathcal{H}_∞ error, for $r = 4, 6$, HNA yields slightly better results. Hence, for this example as well, using interpolatory projections, we are able to beat MBT consistently and yield results comparable to or better than that of HNA. Indeed, this is satisfactory since, as stated in the introduction, for the large-scale settings we are interested in, implementing HNA will be a formidable task, if not impossible.

 Table 6: Relative \mathcal{H}_∞ error norms for the Heat Model

r	IHA	MBT	HNA
2	1.08×10^{-2}	1.66×10^{-2}	1.11×10^{-2}
4	8.92×10^{-4}	1.68×10^{-3}	8.47×10^{-4}
6	2.30×10^{-5}	4.61×10^{-5}	2.07×10^{-5}

As done in the previous examples, we illustrate, in Figure 7, the behavior of the *absolute* \mathcal{H}_∞ -error while optimizing over the d_r -term in both IHA and MBT. In this case, MBT almost gains nothing from the d_r -term modification, as the \mathcal{H}_∞ -error is reduced from 1.0897×10^{-3}

only to 1.0894×10^{-3} , a marginal gain of 0.027%. On the other hand, IHA reduces the \mathcal{H}_∞ -error from 1.26×10^{-3} down to 5.46×10^{-4} , a reduction factor of 56.89%. Once again, this reduction in the error is achieved even when the initial \mathcal{H}_∞ -error is bigger than that of BT, providing a clear illustration of the effectiveness of the d_r -term optimization in the proposed method.

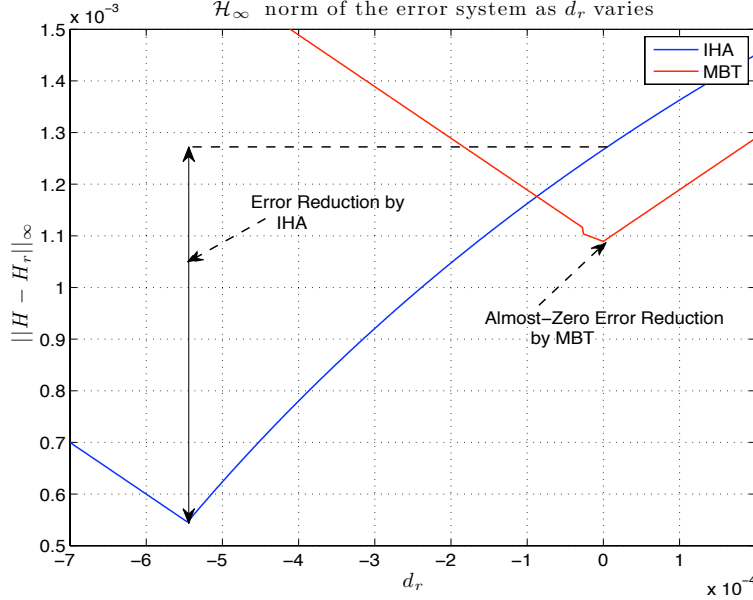


Figure 7: \mathcal{H}_∞ error as a function of the d_r -term in MBT and IHA

To illustrate the importance of using the IRKA points in Step 2 of Algorithm IHA, we use arbitrarily chosen interpolation points (within the bounds of the mirror spectrum of the full order \mathbf{A}) rather than the IRKA points. Then, we apply the same d_r -term modification as before. For $r = 6$, for example, the resulting relative \mathcal{H}_∞ -error is 1.72×10^{-3} , two orders of magnitude higher than what we obtain using the IRKA points. This simple example illustrates the advantage of initializing Step 2 of Algorithm IHA with points computed by IRKA. We want to emphasize that these arbitrary interpolation points are indeed used to initialize IRKA. Hence, IRKA corrects these arbitrarily chosen points, producing interpolation points that are used to obtain an \mathcal{H}_∞ -error norm two orders of magnitude smaller.

4.4 A Heat Transfer Problem for Optimal Cooling of Steel Profiles

This model arises during a cooling process in a rolling mill and is modeled as boundary control of a two dimensional heat equation. The full order model has $n = 79841$ with 7 inputs and 6 outputs. We consider a SISO subsystem corresponding to the sixth input and the second output. For details regarding this model, see [8, 9]. For such a large order, implementing HNA is not possible. BT can be implemented iteratively using ADI-type methods; however

this requires state-of-the-art iterative Lyapunov solvers (two generalized Lyapunov equations of order $n = 79841$ need to be solved) and is not the focus of this paper. Hence, we concentrate only on the performance of the proposed method and compare it with IRKA to show the improvement by the d_r -term optimization. IRKA in Step 1 of Algorithm IHA is implemented in Matlab using direct sparse linear solves. Once again, we illustrate the solution of the optimization problem in Step 2 of Algorithm IHA by both approaches, i.e. directly solving the large-scale optimization problem and using the method of §3.2. The results are shown in Table 7, revealing the same pattern as before. We note that the direct solution of this scalar optimization problem requires several \mathcal{H}_∞ norm computation for a system of order $79841 + r$. As this is not possible to compute exactly, the \mathcal{H}_∞ norms in this direct method are computed approximately by sampling the imaginary axis at 500 points logarithmically spaced points between 10^{-8} and 10. However, this is not an issue for the Loewner matrix approach as the \mathcal{H}_∞ -norm computations are done on systems of order k ; which is less than 13 in this example. The decay of the singular values of $s_i\mathbb{L} - \mathbb{M}$ is shown

Table 7: Solution of the optimization problem in Step 2

r	Exact		Loewner		
	d_r^*	$\ H - H_r^*\ _{\mathcal{H}_\infty}$	d_r^*	$\ H - H_r^*\ _{\mathcal{H}_\infty}$	k
2	1.0189×10^{-2}	6.3715×10^{-1}	1.2685×10^{-2}	6.3725×10^{-1}	7
4	-1.0500×10^{-5}	7.4620×10^{-2}	-5.3232×10^{-5}	7.5483×10^{-2}	12
6	-1.6859×10^{-5}	5.4567×10^{-3}	-1.6849×10^{-5}	5.4592×10^{-3}	13

in Figure 8, illustrating the choice of k . Only the $r = 6$ case is presented; the other cases show the same pattern.

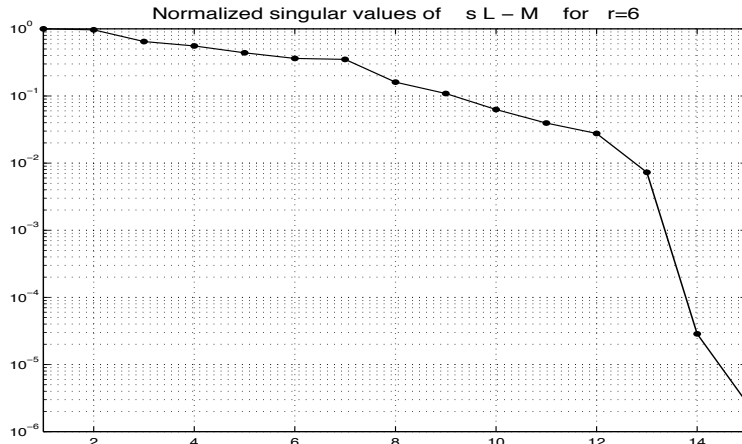


Figure 8: The decay of the singular values of $s_i\mathbb{L} - \mathbb{M}$ for the optimal cooling model

Now, we compare the performance of IHA with that of IRKA for $r = 2, 4, 6$, to illustrate the

gain by the optimization over the d_r -term. The results are listed in Table 8. As expected IHA outperforms IRKA for every r -value.

Table 8: Relative \mathcal{H}_∞ error norms for the Rail Model Order 79841

r	IRKA	IHA
2	6.46×10^{-1}	6.37×10^{-1}
4	1.80×10^{-1}	7.46×10^{-2}
6	1.40×10^{-2}	5.46×10^{-3}

In Figure 9, we demonstrate how the *absolute* \mathcal{H}_∞ error changes over values of d_r , for the order $r = 6$ approximation. In this case, the \mathcal{H}_∞ -error is decreased by over a factor of two, from 2.58×10^{-4} down to 1.09×10^{-4} . We also note that, for $r = 6$, computing the optimal d_r^* term placed an additional interpolation point at 2.44×10^{-2} , yielding exactly $2r + 1 = 13$ interpolation points in \mathbb{C}_+ as suggested by Theorem 3.1. Recalling Theorem 3.1, in Figure 10 we demonstrate how this additional interpolation condition therefore results in a tighter, more circular Nyquist plot, which is equivalent to the image of the error along the imaginary axis being nearly circular.

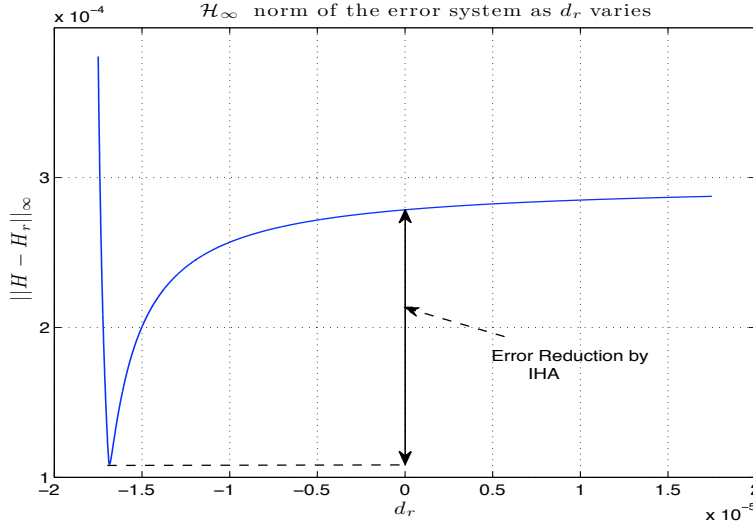


Figure 9: \mathcal{H}_∞ error as a function of the d_r -term

5 Conclusions

We have introduced an interpolation-based model reduction technique to construct high-fidelity \mathcal{H}_∞ approximations for large-scale linear dynamical systems. For a given order

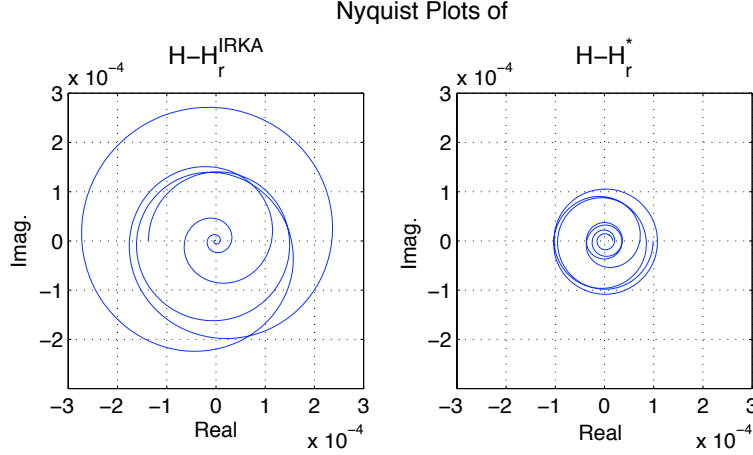


Figure 10: The error curve for H_r^* is nearly circular

r , $2r$ interpolation points are produced using optimal \mathcal{H}_2 approximation. The d_r (feed-forward) term is then adjusted in a such way that these initial $2r$ -interpolation points are kept and an additional interpolation point is added that minimizes the \mathcal{H}_∞ -error norm. By employing a data-driven Loewner matrix approach to model reduction, this optimization step may be performed at negligible cost so that no large-scale \mathcal{H}_∞ -norm computations are ever needed. The main cost of the method is simply solving sparse linear systems. Four numerical examples show that the proposed method produces high fidelity \mathcal{H}_∞ reduced-order models that consistently perform better than those obtained by balanced truncation; and that are as good as (and sometimes better than) those obtained by optimal Hankel norm approximation; in both cases at much lower computational cost.

References

- [1] A.C. Antoulas. *Approximation of Large-Scale Dynamical Systems (Advances in Design and Control)*. Society for Industrial and Applied Mathematics, Philadelphia, PA, USA, 2005.
- [2] A.C. Antoulas and A. Astolfi. \mathcal{H}_∞ -norm approximation. In V.D. Blondel and A. Megretski, editors, *Unsolved Problems in Mathematical Systems and Control Theory*, pages 267–270. Princeton University Press, USA, 2004.
- [3] A.C. Antoulas, D.C. Sorensen, and S. Gugercin. A survey of model reduction methods for large-scale systems. *Contemporary Mathematics*, 280:193–219, 2001.
- [4] A.C. Antoulas, C.A. Beattie, and S. Gugercin. Interpolatory model reduction of large-scale dynamical systems. In J. Mohammadpour and K. Grigoriadis, editors, *Efficient Modeling and Control of Large-Scale Systems*. Springer-Verlag, 2010.

- [5] C. Beattie and S. Gugercin. Interpolatory projection methods for structure-preserving model reduction. *Systems & Control Letters*, 58(3):225 – 232, 2009.
- [6] C.A. Beattie and S. Gugercin. Krylov-based minimization for optimal \mathcal{H}_2 model reduction. *46th IEEE Conference on Decision and Control*, pages 4385–4390, Dec. 2007.
- [7] C.A. Beattie and S. Gugercin. A trust region method for optimal \mathcal{H}_2 model reduction. *48th IEEE Conference on Decision and Control*, Dec. 2009.
- [8] P. Benner. Solving large-scale control problems. *Control Systems Magazine, IEEE*, 24(1):44–59, 2004.
- [9] P. Benner and J. Saak. Efficient numerical solution of the LQR-problem for the heat equation. *Proc. Appl. Math. Mech*, 4(1):648–649, 2004.
- [10] P. Benner, E. S. Quintana-Ortí, and G. Quintana-Ortí. State-Space Truncation Methods for Parallel Model Reduction of Large-Scale Systems. *Parallel Computing, special issue on “Parallel and Distributed Scientific and Engineering Computing”*, 29:1701–1722, 2003.
- [11] P. Benner, E.S. Quintana-Orti, and G. Quintana-Orti. Computing optimal Hankel norm approximations of large-scale systems. In *Proceedings of 43rd IEEE Conference on Decision and Control*, volume 3, pages 3078 – 3083, December 2004.
- [12] Y. Chahlaoui and P. Van Dooren. Benchmark examples for model reduction of linear time-invariant dynamical systems. *Dimension Reduction of Large-Scale Systems*, 45: 381–395, 2005.
- [13] G.M. Flagg. An interpolation-based approach to optimal \mathcal{H}_∞ model reduction. Master’s thesis, Virginia Tech, Department of Mathematics, May 2009.
- [14] K. Glover. All optimal Hankel-norm approximations of linear multivariable systems and their \mathcal{L}_∞ -error bounds. *Int J Control*, 39(6):1115–1193, 1984.
- [15] K.M. Grigoriadis. Optimal \mathcal{H}_∞ model reduction via linear matrix inequalities: continuous- and discrete-time cases. *Systems & Control Letters*, 26(5):321 – 333, 1995.
- [16] E.J. Grimme. *Krylov projection methods for model reduction*. PhD thesis, University of Illinois, 1997.
- [17] S. Gugercin. *Projection methods for model reduction of large-scale dynamical systems*. PhD thesis, Ph. D. Dissertation, ECE Dept., Rice University, 2002.
- [18] S. Gugercin. An iterative rational Krylov algorithm (IRKA) for optimal \mathcal{H}_2 model reduction. In *Householder Symposium XVI*, Seven Springs Mountain Resort, PA, USA, May 2005.

- [19] S. Gugercin and A.C. Antoulas. A survey of model reduction by balanced truncation and some new results. *International Journal of Control*, 77(8):748–766, 2004.
- [20] S. Gugercin, D.C. Sorensen, and A.C. Antoulas. A modified low-rank Smith method for large-scale Lyapunov equations. *Numerical Algorithms*, 32(1):27–55, 2003.
- [21] S. Gugercin, A.C. Antoulas, and C. Beattie. \mathcal{H}_2 model reduction for large-scale linear dynamical systems. *SIAM Journal on Matrix Analysis and Applications*, 30(2):609–638, 2008.
- [22] M. Heinkenschloss, D.C. Sorensen, and K. Sun. Balanced Truncation Model Reduction for a Class of Descriptor Systems with Application to the Oseen Equations. *SIAM Journal on Scientific Computing*, 30:1038, 2008.
- [23] A. Helmersson. Model reduction using LMIs. In *Proceedings of the 33rd IEEE Conference on Decision and Control*, volume 4, pages 3217–3222, December 1994.
- [24] D. Kavranoglu. Zeroth order \mathcal{H}_∞ norm approximation of multivariable systems. *Numerical Functional Analysis and Optimization*, 14(1):89–101, 1993.
- [25] D. Kavranoglu. \mathcal{H}_∞ approximation of discrete-time systems by constant matrices. *Numerical Functional Analysis and Optimization*, 16:177–196, 1995.
- [26] D. Kavranoglu and M. Bettayeb. Characterization of the solution to the optimal \mathcal{H}_∞ model reduction problem. *Systems & Control Letters*, 20(2):99–107, 1993.
- [27] A.R. Kellems, D. Roos, N. Xiao, and S.J. Cox. Low-dimensional, morphologically accurate models of subthreshold membrane potential. *Journal of Computational Neuroscience*, 27(2):161–176, 2009.
- [28] W.Q. Liu, V. Sreeram, and K.L. Teo. Model Reduction for State-space Symmetric Systems. *Systems & Control Letters*, 34:209–215, 1998.
- [29] AJ Mayo and AC Antoulas. A framework for the solution of the generalized realization problem. *Linear Algebra and its Applications*, 425(2-3):634 – 662, 2007.
- [30] L. Meier III and D. Luenberger. Approximation of linear constant systems. *Automatic Control, IEEE Transactions on*, 12(5):585–588, 1967.
- [31] B. Moore. Principal component analysis in linear systems: Controllability, observability, and model reduction. *Automatic Control, IEEE Transactions on*, 26(1):17–32, 1981.
- [32] C. Mullis and R. Roberts. Synthesis of minimum roundoff noise fixed point digital filters. *Circuits and Systems, IEEE Transactions on*, 23(9):551–562, 1976.
- [33] T. Penzl. A cyclic low rank Smith method for large sparse Lyapunov equations. *SIAM Journal on Scientific Comput*, 21(4):1401–1418, 2000.

- [34] T. Reis and T. Stykel. Lyapunov balancing for passivity-preserving model reduction of rc circuits. *SIAM journal on Applied Dynamical Systems*, 10(1):1–34, 2011.
- [35] D.C. Sorensen and A.C. Antoulas. The Sylvester equation and approximate balanced reduction. *Linear algebra and its applications*, 351:671–700, 2002.
- [36] J.T. Spanos, M.H. Milman, and D.L. Mingori. A new algorithm for L^2 optimal model reduction. *Automatica*, 28(5):897–909, 1992.
- [37] B. Srinivasan and P. Myszkorowski. Model reduction of systems with zeros interlacing the poles. *Systems & Control Letters*, 30(1):19–24, 1997.
- [38] T. Stykel. Gramian-Based Model Reduction for Descriptor Systems. *Mathematics of Control, Signals, and Systems (MCSS)*, 16(4):297–319, 2004.
- [39] L.N. Trefethen. Rational Chebyshev approximation on the unit disk. *Numer. Math.*, 37:297–320, 1981.
- [40] P. Van Dooren, K.A. Gallivan, and P.A. Absil. \mathcal{H}_2 -optimal model reduction of MIMO systems. *Applied Mathematics Letters*, 21(12):1267–1273, 2008.
- [41] A. Varga and P. Parrilo. Fast algorithms for solving \mathcal{H}_∞ norm minimization problems. In *Proceedings of the 40th IEEE Conference on Decision and Control*, 2001.
- [42] C.D. Villemagne and R.E. Skelton. Model reduction using a projection formulation. *Intl. J. Contr.*, 46:2141–2169, 1987.
- [43] D.A. Wilson. Optimum solution of model-reduction problem. *Proc. IEE*, 117(6):1161–1165, 1970.
- [44] A. Yousuff and R.E. Skelton. Covariance Equivalent Realizations with Application to Model Reduction of Large Scale Systems. *Control and Dynamic Systems*, 22, 1984.
- [45] A. Yousuff, D.A. Wagie, and R.E. Skelton. Linear system approximation via covariance equivalent realizations. *Journal of mathematical analysis and applications*, 106(1):91–115, 1985.
- [46] B. Yuanqiang and K. Grigoriadis. h_∞ model reduction of symmetric systems using LMIs. In *Decision and Control, 2006 45th IEEE Conference on*, pages 3412–3417, 2006.
- [47] D. Zigic, L.T. Watson, and C.A. Beattie. Contragredient transformations applied to the optimal projection equations. *Linear algebra and its applications*, 188:665–676, 1993.